

A Framework for NLOS Ultra-Wideband Ranging in Collaborative Mobile Robot Systems

Amanda Prorok*, Phillip Tomé** and Alcherio Martinoli*

*Distributed Intelligent Systems and Algorithms Laboratory, School of Architecture, Civil and Environmental Engineering.

**Electronics and Signal Processing Laboratory, School of Engineering.

Ecole Polytechnique Fédérale de Lausanne, Switzerland. Email: firstname.lastname@epfl.ch

Abstract—Ultra-wideband (UWB) localization is one of the most promising indoor localization methods. Yet, non-line-of-sight (NLOS) positioning scenarios remain a challenge and can potentially cause significant localization errors. In this work, we leverage the collaborative paradigm of a multi-robot system by sharing relative positioning information, and thus alleviating error susceptibility in NLOS ranging scenarios. In particular, we detail a decentralized particle filter based localization algorithm which combines an UWB range model with a robot detection model. Finally, we test both collaborative and non-collaborative versions of our algorithm in simulation, in mixed LOS/NLOS scenarios. Results show superior performance for the collaborative system when compared to non-collaborative systems utilizing only UWB ranging.

Index Terms—Collaborative localization, ultra-wideband, mobile robots

I. INTRODUCTION

Accurate indoor localization is an enabling technology. Within the research community, the mobile robotics domain plays an important role with a vast and continuously growing body of contributions. In particular, works completed in recent years have pointed out the advantages of collaborative, multi-robot systems over single-robot systems in terms of localization performance. Indeed, the strategy of multi-robot collaboration is able to compensate for deficiencies in the data owned by a singular robot [1]. Despite the outstanding features of UWB for positioning, such as good penetrability through objects and high accuracy, the signal remains affected by multipath problems requiring complex range estimation algorithms to maintain theoretically optimal performances [10]. Thus, our ultimate goal is to mitigate these effects and optimize localization accuracy by including information provided by other team-members.

In this paper, we consider the problem of absolute localization of a team of mobile robots for unknown initial pose estimates in a common frame. We design an algorithm targeting miniaturized, computationally limited platforms equipped with noisy, low-power sensing modalities. Given its efficiency in solving localization problems for unknown initial conditions, and for accommodating arbitrary probability density functions, our method of choice is the particle filter, building on the probabilistic framework of Monte-Carlo Localization (MCL) presented in [1]. Our localization strategy uses range measurements from one UWB base-station, relative (inter-robot)

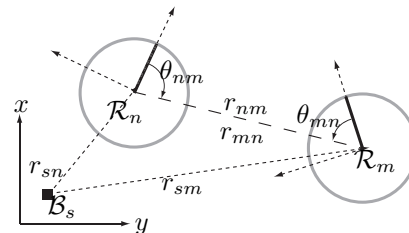


Fig. 1. System of two robots (\mathcal{R}_n and \mathcal{R}_m) sharing a common localization frame. The figure illustrates the robots' relative range (r_{nm} and r_{mn}) and bearing (θ_{nm} and θ_{mn}) values. A UWB base-station is marked by \mathcal{B}_s , and ranges to the individual robots are shown (r_{sn} and r_{sm}).

observations, and a common map of the environment a priori available on each robot.

A. Related Work

UWB has shown to be amongst the most promising localization techniques for indoor environments [4]. In consequence, it has very recently been adopted by the robotics community. In [11], an UWB receiver is mounted on a mobile robot which uses a time-difference-of-arrival (TDOA) algorithm between pairs of anchor nodes to estimate its own position. The robot's self-localization algorithm is based on UWB measurements only, and no sensor fusion is considered. Further, the studies in [2] and [3] develop probabilistic models for biased UWB range measurements which are combined with onboard odometry data. Yet, given the novelty of UWB positioning systems in the robotics community, to the best of our knowledge, no significant studies have been performed on the fusion of UWB with onboard exteroceptive sensors, in the case of single-robot systems, nor any onboard relative positioning sensors, in the case of multi-robot systems.

B. Problem Formulation

Our problem is described as follows. We have a multi-robot system of N robots $\mathcal{R}_1, \mathcal{R}_2, \dots, \mathcal{R}_N$, where the number N does not need to be known by the robots. The robots navigate in a common frame in a space bounded by a map; for a robot \mathcal{R}_n , at time t , the pose $\mathbf{x}_{n,t}$ is given by the Cartesian coordinates $x_{n,t}, y_{n,t}$ and orientation $\phi_{n,t}$. Also, at time t , a robot \mathcal{R}_m is in the set of neighbors $\mathcal{N}_{n,t}$ of robot \mathcal{R}_n if robot \mathcal{R}_m can determine a range $r_{mn,t}$ and bearing $\theta_{mn,t}$ to robot \mathcal{R}_n . We make the assumption that a robot \mathcal{R}_m can communicate with a robot \mathcal{R}_n , if $\mathcal{R}_m \in \mathcal{N}_{n,t}$. Furthermore, every robot \mathcal{R}_n in the system receives a range r_{sn} from the base-station \mathcal{B}_s , which is fixed and well-localized in the absolute coordinate system. Apart from these sensing modalities, the robots are

This work was sponsored by the National Center of Competence in Research on Mobile Information and Communication Systems under grant number 51NF40-111400.

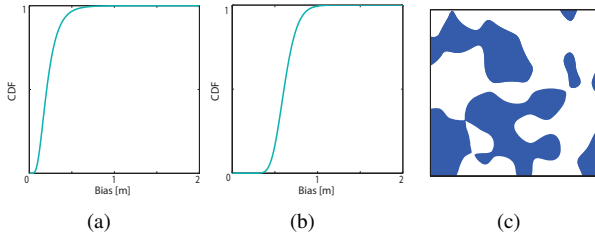


Fig. 2. Cumulative density function of a log-normal bias with (a) $\mu_{\ln\mathcal{N}} = -1.59$, $\sigma_{\ln\mathcal{N}} = 0.49$ and (b) with $\mu_{\ln\mathcal{N}} = -0.5$, $\sigma_{\ln\mathcal{N}} = 0.2$. (c) Example 9m^2 large area with a LOS/NLOS mixing ratio of 1/1.

also equipped with a dead-reckoning self-localization module (e.g. wheel-based odometry). Given these specifications, the goal is to localize all robots, without any prior knowledge of their initial pose or previous measurements.

II. UWB RANGE ERROR MODEL

UWB is a radio technology which is characterized by its very large bandwidth compared to conventional narrowband systems, and in particular features high positioning accuracy (due to a high time resolution) and high material penetrability (due to the large bandwidth). Despite these desirable traits, the resolution of multipath signals leads to complex TOA algorithms prone to estimation errors, which inevitably leads to ranging inaccuracies. In this paper, we employ a popular error model [10] for the range between a base-station \mathcal{B}_s and a target node \mathcal{R}_n

$$\hat{r}_{sn} = r_{sn} + b_{sn} + \epsilon_{sn} \quad (1)$$

where r_{sn} represents the true distance, b_{sn} is a non-negative distance bias introduced by a NLOS signal propagation, and $\epsilon_{sn} \sim \mathcal{N}(0, \sigma_{\mathcal{N}}^2)$ is a zero-mean Gaussian measurement noise with variance $\sigma_{\mathcal{N}}^2$. Whereas modeling ϵ_{sn} is straightforward, modeling the bias b_{sn} is less obvious. Current work discusses a variety of viable statistical models with exponential behavior [6, 9]. Indeed, biases may not only be caused by multipath propagation, but also by signal delay or by signal attenuation, and thus are dependent on bandwidth and distance. Despite the complexity of NLOS error patterns, we resort to a statistical model, the log-normal distribution, as it is shown to best characterize the spatial NLOS error behavior in the comprehensive measurement campaign of [6]. Furthermore, we recreate a mixed LOS/NLOS area by defining random patches where range measures are consistently affected by a bias drawn from a log-normal distribution $b_{sn} \sim \ln\mathcal{N}(\mu_{\ln\mathcal{N}}, \sigma_{\ln\mathcal{N}})$. Figures 2(a) and 2(b) show the cumulative density functions employed in this paper, (a) for a mild bias with $\mu_{\ln\mathcal{N}} = -1.59$, $\sigma_{\ln\mathcal{N}} = 0.49$ (as for the Schussler system of [6]) and (b) for a harsh bias with $\mu_{\ln\mathcal{N}} = -0.5$, $\sigma_{\ln\mathcal{N}} = 0.2$. Figure 2(c) shows an example 9m^2 large area with a spatial LOS/NLOS mixing ratio of 1/1.

III. COLLABORATIVE MONTE-CARLO LOCALIZATION

In this section, we briefly review Monte-Carlo Localization (MCL), as it forms a baseline for our work. We then extend the standard MCL formalism to a fully decentralized, collaborative adaptation resulting in the complete routine as shown in

Algorithm 1. Let us from hereon consider a robot \mathcal{R}_n . At time t , after a sequence of motion control actions $u_{n,t}$ and a sequence of observations $z_{n,t}$ the recursive update equation is denoted

$$\mathbf{Bel}(\mathbf{x}_{n,t}) = \eta p(z_{n,t}|\mathbf{x}_{n,t}) \int p(\mathbf{x}_{n,t}|\mathbf{x}_{n,t-1}, u_{n,t-1}) \mathbf{Bel}(\mathbf{x}_{n,t-1}) d\mathbf{x}_{n,t-1} \quad (2)$$

where $\mathbf{Bel}(\mathbf{x}_{n,t})$ estimates of the posterior state $\mathbf{x}_{n,t}$ and is called a *belief*. The value η is a normalization constant, $p(z_{n,t}|\mathbf{x}_{n,t})$ is the measurement model, and $p(\mathbf{x}_{n,t}|\mathbf{x}_{n,t-1}, u_{n,t-1})$ the motion model.

The main idea of MCL lies in the way the belief is represented—samples, or particles, are drawn from the posterior probability distribution of the robot pose to form a set of particles. By weighting these particles one obtains a discrete probability function that approximates the continuous belief $\mathbf{Bel}(\mathbf{x}_{n,t})$, and hence we have

$$\mathbf{Bel}(\mathbf{x}_{n,t}) \sim \{\langle \mathbf{x}_{n,t}^{[i]}, w_{n,t}^{[i]} \rangle | i = 1, \dots, M\} = X_{n,t} \quad (3)$$

where M is the number of particles, $\mathbf{x}_{n,t}^{[i]}$ is a sample of the random variable $\mathbf{x}_{n,t}$ (the pose), and $w_{n,t}^{[i]}$ is its weight.

The framework presented above takes into account a single robot. However, when operating a collaborative multi-robot system, the baseline formalism must be adapted to integrate measurements taken on different platforms [1]. If we make the assumption that individual robot poses are independent, we can formulate the event that robot \mathcal{R}_n is detected by robot \mathcal{R}_m as

$$\mathbf{Bel}(\mathbf{x}_{n,t}) = p(\mathbf{x}_{n,t}|z_{n,0..t}, u_{n,0..t}) \int p(\mathbf{x}_{n,t}|\mathbf{x}_{m,t}, r_{mn,t}, \theta_{mn,t}) \mathbf{Bel}(\mathbf{x}_{m,t}) d\mathbf{x}_{m,t} \quad (4)$$

where $p(\mathbf{x}_{n,t}|z_{n,0..t}, u_{n,0..t})$ describes the n^{th} robot's current belief, and $\int p(\mathbf{x}_{n,t}|\mathbf{x}_{m,t}, r_{mn,t}, \theta_{mn,t}) \mathbf{Bel}(\mathbf{x}_{m,t}) d\mathbf{x}_{m,t}$ describes the m^{th} robot's belief about the position of robot \mathcal{R}_n . For such a collaboration to take place, robot \mathcal{R}_m needs to communicate $r_{mn,t}, \theta_{mn,t}$ and $\mathbf{Bel}(\mathbf{x}_{m,t})$ to robot \mathcal{R}_n . Thus a communication message is composed as $d_{mn,t} = \langle r_{mn,t}, \theta_{mn,t}, X_{m,t} \rangle$. If several robots in a neighborhood $\mathcal{N}_{n,t}$ communicate with robot \mathcal{R}_n , the received information is the set of all communication messages $D_{n,t} = \{d_{mn,t} | \mathcal{R}_m \in \mathcal{N}_{n,t}\}$. We note that the collaborative aspect of this formalism lies in the integration of robot \mathcal{R}_m 's belief into that of robot \mathcal{R}_n . This update step is shown in Algorithm 1 (line 5). Finally, we complete our algorithm with a collaborative, *reciprocal* sampling routine, which at each update step adds a proportion α of particles drawn from the distribution $\mathbf{x}_{n,t}^{[i]} \sim p(D_{n,t}|\mathbf{x}_{n,t}^{[i]})$ according to the robot detection model. This additional technique accounts for the collapse of particles onto one pose estimate given a finite number of particles. The reciprocal sampling algorithm is elaborated in more detail, later in Section IV-B.

IV. OBSERVATION MODELS

In the following two paragraphs, we describe the TOA measurement model applied to UWB ranging, and a detection model, applied to the relative range and bearing observations.

Algorithm 1 MultiRobot_MCL($X_{n,t-1}, u_{n,t}, \hat{r}_{n,t}, D_{n,t}$)

```
1:  $\bar{X}_{n,t} = X_{n,t} = \emptyset$ 
2: for  $i = 1$  to  $M$  do
3:    $\mathbf{x}_{n,t}^{[i]} \leftarrow \text{Motion\_Model}(u_{n,t}, \mathbf{x}_{n,t-1}^{[i]})$ 
4:    $w_{n,t}^{[i]} \leftarrow \text{Measurement\_Model}(\hat{r}_{n,t}, \mathbf{x}_{n,t}^{[i]})$ 
5:    $w_{n,t}^{[i]} \leftarrow \text{Detection\_Model}(D_{n,t}, \mathbf{x}_{n,t}^{[i]}, w_{n,t}^{[i]})$ 
6:    $\bar{X}_{n,t} \leftarrow \bar{X}_{n,t} + \langle \mathbf{x}_{n,t}^{[i]}, w_{n,t}^{[i]} \rangle$ 
7: end for
8: for  $i = 1$  to  $M$  do
9:    $r \sim \mathcal{U}(0, 1)$ 
10:  if  $r \leq (1 - \alpha)$  then
11:     $\mathbf{x}_{n,t}^{[i]} \leftarrow \text{Sampling}(\bar{X}_{n,t})$ 
12:  else
13:     $\mathbf{x}_{n,t}^{[i]} \leftarrow \text{Reciprocal\_Sampling}(D_{n,t}, \bar{X}_{n,t})$ 
14:  end if
15:   $X_{n,t} \leftarrow X_{n,t} + \langle \mathbf{x}_{n,t}^{[i]}, w_{n,t}^{[i]} \rangle$ 
16: end for
17: return  $X_{n,t}$ 
```

A. TOA Measurement Model

The TOA measurement model returns the likelihood that a robot \mathcal{R}_n measures a certain range distance \hat{r}_{sn} from a beacon \mathcal{B}_s at a position $\mathbf{x}_{n,t}$. We denote the event of a LOS path at location \mathbf{x}_n of beacon \mathcal{B}_s as L_{sn} , and the event of a NLOS path \bar{L}_{sn} , respectively. For a log-normal probability density function $P_{ln\mathcal{N}}(b)$ with parameters $\mu_{ln\mathcal{N}}$ and $\sigma_{ln\mathcal{N}}$, and a normal probability density function $P_{\mathcal{N}}(\epsilon)$ with a standard deviation $\sigma_{\mathcal{N}}$, we define the probability of measuring a range in a NLOS condition as

$$P_{sn}(\mathbf{x}_n | \hat{r}_{sn}, \bar{L}_{sn}) = \int P_{ln\mathcal{N}}(b) \cdot P_{\mathcal{N}}(\epsilon_{sn} = \hat{r}_{sn} - r_{sn} - b) db$$

which is the convolution of the probability density function of the bias value, with the probability density function of the white noise value. Correspondingly, we define the probability of measuring a range in a LOS condition as

$$P_{sn}(\mathbf{x}_n | \hat{r}_{sn}, L_{sn}) = P_{\mathcal{N}}(\epsilon = \hat{r}_{sn} - r_{sn}). \quad (5)$$

Finally, with use of the total probability theorem, we combine the above equations to obtain the probability of measuring a range \hat{r}_{sn}

$$P_{sn}(\mathbf{x}_n | \hat{r}_{sn}) = P_{sn}(\mathbf{x}_n | \hat{r}_{sn}, L_{sn}) \cdot P_{L_{sn}} + P_{sn}(\mathbf{x}_n | \hat{r}_{sn}, \bar{L}_{sn}) \cdot (1 - P_{L_{sn}}) \quad (6)$$

where $P_{L_{sn}}$ is the probability of measuring a LOS path, and correspondingly, $(1 - P_{L_{sn}})$ is the probability of measuring a NLOS path. Indeed, in this work we assume no a-priori knowledge about $P_{L_{sn}}$ for all \mathbf{x}_n , and an additional model must be devised with the purpose of estimating it. Finally, the TOA measurement model can be formulated as an update equation as shown in Algorithm 2.

Figure 3 shows an application of Equation 6, weighting particles in (a) a LOS scenario and (b) a NLOS scenario, for a single base-station, where the probability of $P_{L_{sn}}$ is known (in this case we have (a) $P_{L_{sn}} = 1$ and (b) $P_{L_{sn}} = 0$).

Algorithm 2 Measurement_Model($\hat{r}_{n,t}, \mathbf{x}_t^{[i]}$)

```
1:  $w \leftarrow \prod_{s \in \mathcal{B}_s} P_{sn}(\mathbf{x}_t^{[i]} | \hat{r}_{sn})$ 
2: return  $w$ 
```

Algorithm 3 Detection_Model($D_{n,t}, \mathbf{x}_t^{[i]}, w_t^{[i]}$)

```
1:  $w \leftarrow w_t^{[i]} \cdot \prod_{d_{mn} \in D_{n,t}} P_{mn}(\mathbf{x}_t^{[i]} | d_{mn})$ 
2: return  $w$ 
```

B. Range & Bearing Detection Model

The idea of the range and bearing model is to propose a probability density function which is based on the relative observations made by the detection sensors, and which is also based on the belief of the detecting robot. We then simultaneously use this probability density function as an observation model in the belief update, and as a proposal distribution for the reciprocal sampling routine.

For clarity, we omit the subscript t in the following derivations. A robot \mathcal{R}_m detects a robot \mathcal{R}_n with a range r_{mn} and relative bearing θ_{mn} . We formulate the detection model as $P_{mn}(\mathbf{x}_n | d_{mn})$ which describes the probability that robot \mathcal{R}_m detects robot \mathcal{R}_n at pose $\mathbf{x}_n = [x_n \ y_n \ \phi_n]$, given the detection data d_{mn} . For a given particle i in robot \mathcal{R}_m 's belief, we define the range difference Δr_{mn} , and the bearing difference $\Delta \theta_{mn}$. The range and bearing differences are given by the geometric relations

$$\begin{aligned} \Delta r_{mn} &= \sqrt{\Delta x_{mn}^2 + \Delta y_{mn}^2} - r_{mn} \\ \Delta \theta_{mn} &= \text{atan2}(\Delta y_{mn}, \Delta x_{mn}) - (\phi_m^{[i]} + \theta_{mn}) \end{aligned}$$

where we denote $\Delta x_{mn} = (x_m^{[i]} - x_n)$ and $\Delta y_{mn} = (y_m^{[i]} - y_n)$. Assuming Gaussian noise and knowledge of the range and bearing standard deviation (σ_r and σ_θ , respectively), and the independence of range and bearing measurements, the detection probability is

$$P_{mn}(\mathbf{x}_n | d_{mn}) = \eta \cdot \sum_{\langle \mathbf{x}_m^{[i]}, w_m^{[i]} \rangle \in X_m} \Phi \left(\begin{bmatrix} \Delta r_{mn} \\ \Delta \theta_{mn} \end{bmatrix}, \begin{bmatrix} \sigma_r^2 & 0 \\ 0 & \sigma_\theta^2 \end{bmatrix} \right) \cdot w_m^{[i]} \quad (7)$$

where $\Phi(\cdot, \Sigma)$ is the zero-mean multivariate normal probability distribution with the covariance matrix Σ and where η is a

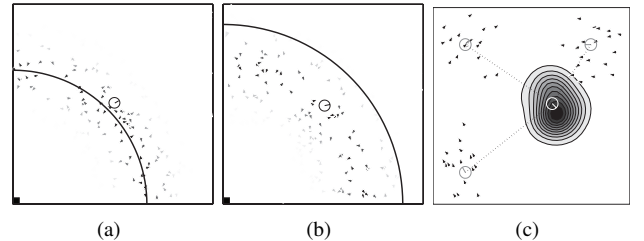


Fig. 3. Illustration of observation models within a particle filter. The pose estimates (particles) are represented by triangles with increasing transparency for decreasing weights. The dashed line represents the noisy/biased range measurement, the robot body shows the actual robot position. TOA measurement model for a single base-station in a (a) LOS scenario (b) NLOS scenario. Robot detection model for 3 detecting robots is shown in (c); the detected robot is shown in white. The model's probability density is superimposed on the detected robot.

normalization constant. Finally, the detection model can be formulated as an update equation as shown in Algorithm 3. Algorithm 4 shows how samples are drawn from the detection model in a reciprocal sampling routine. Figure 3(c) shows an illustration of the probability density function resulting from the detection model for three detecting robots.

Algorithm 4 Reciprocal_Sampling($D_{n,t}, \bar{X}_{n,t}$)

```

1: if  $D_{n,t} = \emptyset$  then
2:    $\mathbf{x} \leftarrow \text{Sampling}(\bar{X}_{n,t})$ 
3: else
4:    $\mathbf{x} \sim \prod_{d_{mn} \in D_{n,t}} P_{mn}(\mathbf{x}|d_{mn})$ 
5: end if
6: return  $\mathbf{x}$ 

```

V. RESULTS

We run our algorithm in a submicroscopic embodied robot simulator (Webots, [5]), employing a model of the Khepera III robot [7] with realistically calibrated sensors and actuators (including a realistic simulation of the hardware range and bearing module [8] with noise values experimentally determined on our actual hardware setup: $\sigma_r = 0.15 \cdot r_{mn}$, and $\sigma_\theta = 0.15\text{rad}$). Our setup consists of a 3m large square arena containing no obstacles (other than the robots themselves, which can occlude and thus prohibit relative range and bearing measurements). At the start of each experiment, the robots are randomly placed in the arena. For all experiments, the robots move straight at a speed of one robot-size per second (12cm/s) and avoid collisions. The simulated TOA range values \hat{r}_{sn} (Eq. 1) are perturbed with a Gaussian noise component $\epsilon_{sn} \sim \mathcal{N}(0, \sigma_{\mathcal{N}}^2)$ with a zero mean and standard deviation $\sigma_{\mathcal{N}} = 0.022\text{m}$ (empirical LOS noise in [6]) and a bias drawn from a log-normal distribution, considering both a mild and a harsh case (as detailed in Section II). The LOS/NLOS proportion is 1/1, and is defined spatially based on a randomly drawn bias map (see Figure 2(c)). TOA range measurements as well as relative observations are made at a frequency of 1Hz.

In order to assess the performance of the collaborative framework, we perform two sets of experiments:

Collaborative 4 collaborative robots with relative observation data, UWB range data, and odometry.

Non-collaborative 4 non-collaborative robots with only UWB range data and odometry.

Each of the two experiment sets is tested on a set of three case-studies, analyzing the impact of knowledge on $P_{L_{sn}}$:

None No knowledge available; no NLOS paths are assumed and $P_{L_{sn}} = 1, \forall s, n$

Naive No knowledge available; a naive assumption is made, i.e. $P_{L_{sn}} = 0.5, \forall s, n$

Optimal Ground truth knowledge is available; $P_{L_{sn}}$ is employed optimally at all times.

Each robot is equipped with a set of 500 particles. We perform 800 runs, each lasting 4min, and log positioning data at a frequency of 2Hz. We discuss the localization performance in terms of the mean positioning error of all particles in a given robot's belief (RMSE). Figure 4 shows the empirical cumulative density function of the RMSE distribution over all runs. For optimal knowledge of $P_{L_{sn}}$, 95.5% of the time

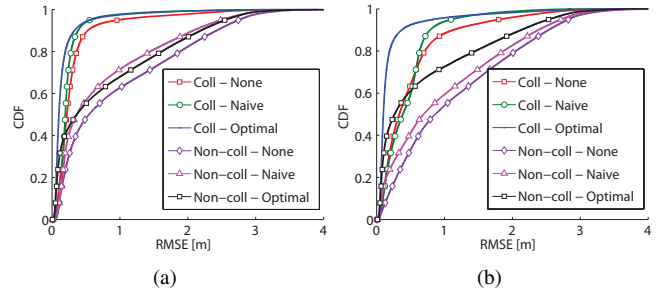


Fig. 4. Cumulative density function of the RMSE distribution over 800 runs, each of 4min duration, (a) for a mild bias and (b) for a harsh bias.

the error of the collaborative system is below 0.61m (mild scenario) and 0.93m (harsh scenario), in comparison to errors of 2.59m and 2.58m, respectively, for the non-collaborative system. Indeed, by imposing additional geometric constraints through the relative observations, the collaborative robot team is more likely to converge to correct position estimates. Also, for any robot which has an approximate estimate of its true position, the propagation of this belief to its team-members will accelerate the process of localizing the whole system.

VI. CONCLUSION

In this work, we presented a scalable, decentralized particle filter algorithm for collaborative localization in mixed LOS/NLOS scenarios. The algorithm has shown that collaboration, through skillful exchange of positioning information, can lead to a clearly improved performance.

REFERENCES

- [1] D. Fox, W. Burgard, H. Kruppa, and S. Thrun. A probabilistic approach to collaborative multi-robot localization. *Autonomous Robots*, 8:325–344, 2000.
- [2] J. González, J. Blanco, C. Galindo, A. O. de Galisteo, J. Fernández-Madrigo, F. Moreno, and J. Martínez. Mobile robot localization based on ultra-wide-band ranging: A particle filter approach. *Robotics and Autonomous Systems*, 57(5):496 – 507, 2009.
- [3] D. Jourdan, J. Deyst, J.J., M. Win, and N. Roy. Monte carlo localization in dense multipath environments using uwb ranging. In *IEEE International Conference on Ultra-Wideband (ICU)*, pages 314–319, 2005.
- [4] H. Liu, H. Darabi, P. Banerjee, and J. Liu. Survey of wireless indoor positioning techniques and systems. *IEEE Transactions on Systems, Man and Cybernetics*, 37(6):1067–1080, 2007.
- [5] O. Michel. Webots: Professional mobile robot simulation. *Journal of Advanced Robotic Systems*, 1(1):39–42, 2004.
- [6] K. P. N. Alsindi, B. Alavi. Measurement and modeling of ultrawideband TOA-based ranging in indoor multipath environments. *IEEE Transactions on Vehicular Technology*, 58:1046–1058, 2009.
- [7] A. Prorok, A. Arfire, A. Bahr, J. Farserotu, and A. Martinoli. Indoor navigation research with the Khepera III mobile robot: An experimental baseline with a case-study on ultra-wideband positioning. In *International Conference on Indoor Positioning and Indoor Navigation (IPIN)*, 2010. doi: 10.1109/IPIN.2010.5647880.
- [8] J. Pugh, X. Raemy, C. Favre, R. Falconi, and A. Martinoli. A fast on-board relative positioning module for multi-robot systems. *IEEE Transactions on Mechatronics*, 14(2):151–162, 2009.
- [9] Y. Qi. *Wireless geolocation in a non-line-of-sight environment*. PhD thesis, Princeton University, 2004.
- [10] Z. Sahinoglu, S. Gezici, and I. Guvenc. *Ultra-wideband Positioning Systems. Theoretical Limits, Ranging Algorithms, and Protocols*. Cambridge University Press, 2008.
- [11] M. Segura, H. Hashemi, C. Sisterna, and V. Mut. Experimental demonstration of self-localized ultra wideband indoor mobile robot navigation system. In *International Conference on Indoor Positioning and Indoor Navigation (IPIN)*, 2010. doi: 10.1109/IPIN.2010.5647457.